TR5.1.5: Report on specially designed components

VALIDATION OF A DYNAMIC MODEL FOR UNGLAZED COLLECTORS INCLUDING CONDENSATION

SP Technical Research Institute of Sweden

Peter Kovács, peter.kovacs@sp.se, phone: +46 10 516 56 62

Version 1

Date: 2012-05-14

Final Document

QAiST is supported by:

INTELLIGENT ENERGY EUROPE

Project IEE/08/593/SI2.529236

Contents

1. Introduction

Unglazed collectors are commonly used for pool heating where the temperature demand is low. The reason is that the simple design of an unglazed collector results in a very favorable energy cost. The use of ground source heat pumps is expanding and in many cases the storage needs more recharging than the natural energy flow from the surroundings can give. In this application the operating temperature will be extremely low, even below the dew point of the air and also 24 hour operation can be possible. To model this operation mode of a solar collector this work has been done to find a solution where an existing model for standardized testing can be upgraded with some correction terms instead of starting from scratch with a new model.

The model validation work has been done by Bengt Perers, Department of Civil Engineering, Technical University of Denmark, Kgs. Lyngby, Denmark and Dalarna University Borlänge Sweden in cooperation with SP Technical Research Institute of Sweden and ÅF Infrastructure Stockholm Sweden. SP has made specially adapted instrumentations and tests for this analysis within the framework of the European IEE project Qaist. ÅF has supported the work and implemented the model in IDA and participated in the model validation work for IDA. In an early stage of this modeling and validation work also the heat pump manufacturer IVT in Sweden supported the experimental work at Lund University.

Some pictures of the collector sample and the test rig at SP in Borås are shown below. The test object was a flat plate unglazed collector made of polymeric materials. It was mounted on a 45 degree tilted surface. Sensors were installed as close as possible to the collector without disturbing the performance. New high class sensors for humidity, ambient temperature and wind speed were added to the standard test equipment for unglazed collectors. Some of the sensors were doubled on each side of the collector.

Figure 1. The unglazed solar collector on the test stand with extra sensors for humidity, wind speed and air temperature. Also sensors for solar radiation and long-wave thermal sky radiation in the collector plane can be seen to the right of the collector. In the upper right corner a new kind of wind sensor is located. **(Photo from SP)**

Figure 2. Close up of the collector absorber surface during condensation operation. A lot of water is "produced" so it is important to have a really water tight roof under the collector. Here the inactive round welding spots on the absorber can be seen too. This affects the parameter values somewhat from the ideal numbers. **(Photo from SP)**

Figure 3. Close up of the absorber showing the connecting pipe and header along the left side of the collector. The mounting screws to the roof can also be seen. It is assumed while modeling that no large amount of air flow can go behind the collector, so that a one sided operation/condensation can be expected. In a real situation a "two sided" mounting arrangement allowing air behind the collector may increase the performance during low temperature operation. (Photo from SP)

2. Model Theory

The EN12975 dynamic collector model is used in the validation work. As this basic model does not consider condensation yet in the standard an extra term is added for this energy flow. This term becomes active when very low operating temperatures are applied. This model then covers an extreme range of collectors from high concentrating or vacuum tube collectors to extreme low temperature unglazed collectors.

$$q = F'(\tau\alpha)_{en} K_{\theta b}(\theta_L,\theta_T)G_b + F'(\tau\alpha)_{en} K_{\theta d}G_d - c_6\, u\, G_T - c_1 (t_m - t_a) - c_2 (t_m - t_a)^2 - c_3\, u\,(t_m - t_a) +$$
$$+ c_4 (E_L - \sigma T_a^4) - c_5\, dt_m/d\tau - c_7 (2.8 - 3.0\, u)(\nu_a - \nu_{sat}(t_m))$$
(eq. 1)

Variables in eq. 1

G_b = beam solar radiation in the collector plane [W/m2]

G_b = diffuse solar radiation in the collector plane [W/m2]

G_T = total (beam + diffuse) solar radiation in the collector plane [W/m2]

θ_L, θ_T = Incidence angles for beam radiation onto the collector plane in longitudinal and transversal direction from the normal.

u = wind speed in the collector plane [m/s]

$t_m = (t_{in} + t_{out})$ 0.5 arithmetic mean fluid temperature between inlet and outlet of the collector [°C]

E_L = long wave or thermal radiation (incident from sky + ambient) in the collector plane [W/m2]

T_a = ambient temperature close to the collector (in the shade) [K] (only radiation calculations)

t_a = ambient temperature close to the collector (in the shade) [°C]

ν_a = absolute humidity of air (derived from measured relative humidity and ambient air temp) [kg/m^3]

$\nu_{sat}(t_m)$ = calculated saturated absolute humidity, of the ambient air, at temperature t_m [kg/m^3]

τ = time during measurements and simulation.

Parameters in eq 1:

$F'(\tau\alpha)_{en}$ = zero loss efficiency of the collector, at normal incidence

$K_{\theta b}(\theta_L,\theta_T)$ = incidence angle modifier for beam solar radiation. $K_{\theta b}$ varies with incidence angles θ, θ_L and θ_T. Note that for many collector designs like concentrating collectors, vacuum tube´s or CPC´s, $K_{\theta b}(\theta)$ is generalised to $K_{\theta b}(\theta_{L,}\ \theta_T)$ where $\theta_{L,}$ and θ_T are transversal and longitudinal incidence angles.

$K_{\theta d}$ = incidence angle modifier for diffuse solar radiation (assumed to be a fixed value for each collector design). This value can be either determined experimentally in a dynamic test or integrated from beam incidence angle modifier curves [24].

c_1 = heat loss coefficient at $(t_m - t_a) = 0$ equal to $F´U_0$ [W/(m2 K)]

c_2 = temperature dependence in the heat loss coefficient equal to $F´U_1$ [$W/(m^2\ K^2)$]

c_3 = wind speed dependence of the heat losses equal to $F´U_{wind}$ [$J/(m^3\ K)$]

c_4 = long wave irradiance dependence of the heat losses, equal to $F´\varepsilon$ [–]

c_5 = effective thermal capacitance, equal to $(mC)_e$ [J/(m2 K)]

c_6 = wind dependence of the zero loss efficiency, a collector constant [s/m]

c_7 = humidity factor of collector [J/kg]. Ideally equal to $r_w / (\rho_{air}\ c_{p\_air}\ Le^{(1-n)})$ for a flat surface and the back side insulated. In reality, the value will depend on the collector design and especially the absorber.

3. Test Results

3.1 Example of collector output power validation results from September 24 –October 14

Figure 4 and 5 show model validation results. Note that 24 hour operation is applied with also negative collector output power. This was to stress the model and check the heat loss modeling. *No selection of data was applied. No correction for wet collector absorber surface due to rain was possible, as this information is not available in raw data.* 5 minute average values are shown. Less condensation operation.

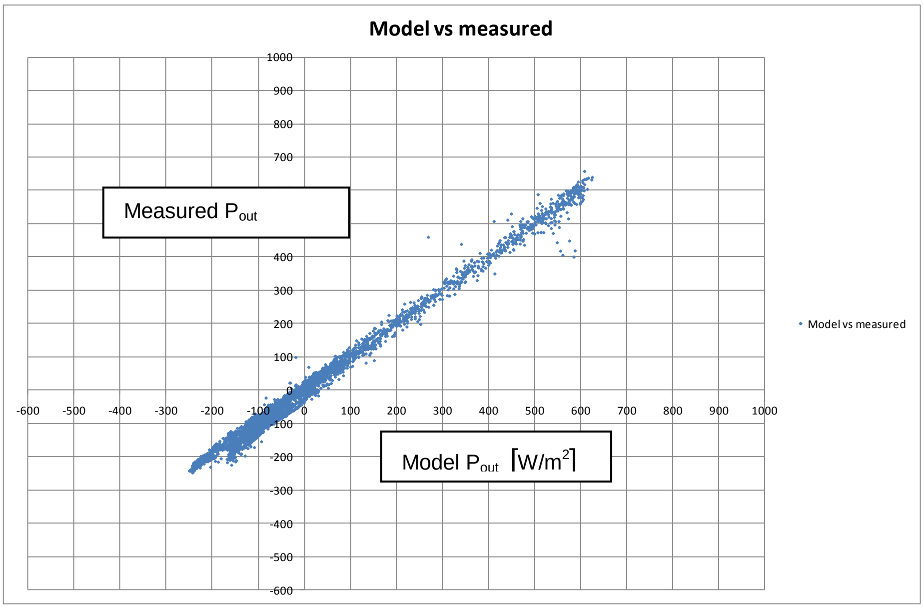

Figure 4. Data from 2010 09 24 to 2010 10 14. 5 minute values. Less condensation operation.

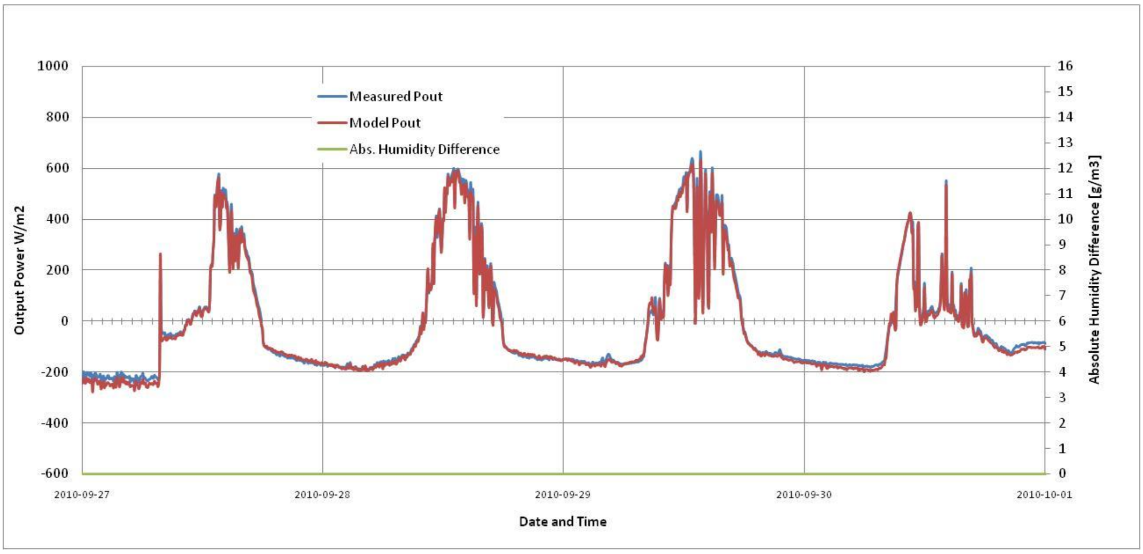

Figure 5. Example of output power data from 2010 09 27 until 2010 10 01. 5 minute average values. No condensation operation in this period. Red= modeled Pout, Blue = measured Pout.

3.2 Example of collector output power validation results from September 8 – September16

In this period more condensation is present see figure 7. Still the model works accurately.

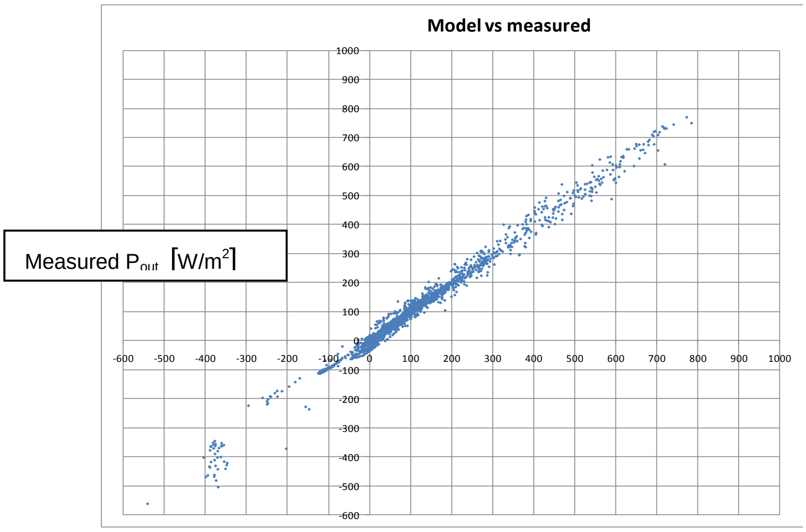

Figure 6. From 2010 09 08 until 2010 09 16. [illegible] values. More condensation ope[illegible]

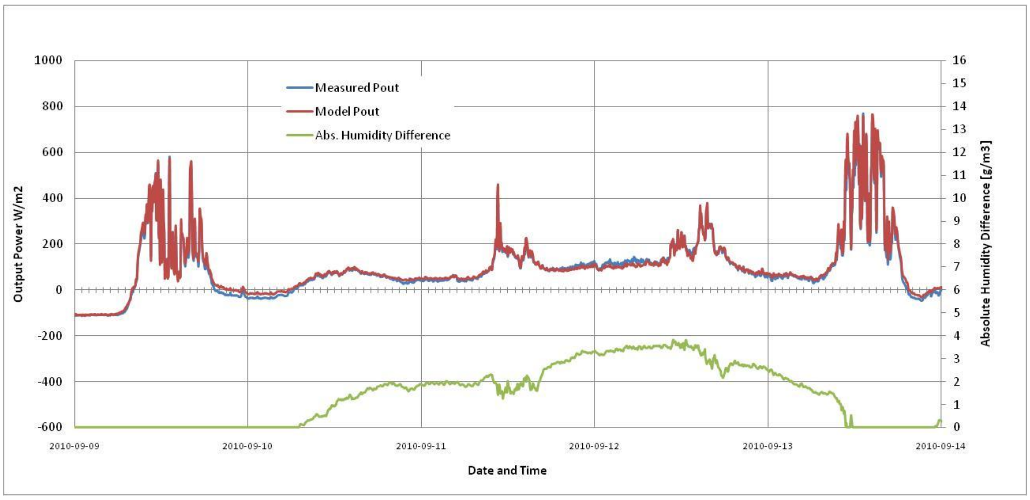

Figure 7. Example of output power data from 2010 09 09 until 2010 09 14 . 5 minute average values. Red= modeled Pout, Blue = measured Pout, Green= absolute humidity difference. High green values correspond to a large amount of condensation.

3.3 All data from September 8 until October 14. 2010

Model versus measurements for the whole test period from September 8 to October 14 are shown in figures 8 and 9. All data day and night are shown. The large scatter is mostly caused by rain onto the collector that evaporates and reduces the output power for short periods. The model can handle this but there is no information about rain in the test data in this data set so this has no correction term in the model here. (Rainy weather can be deduced from the long wave radiation data)

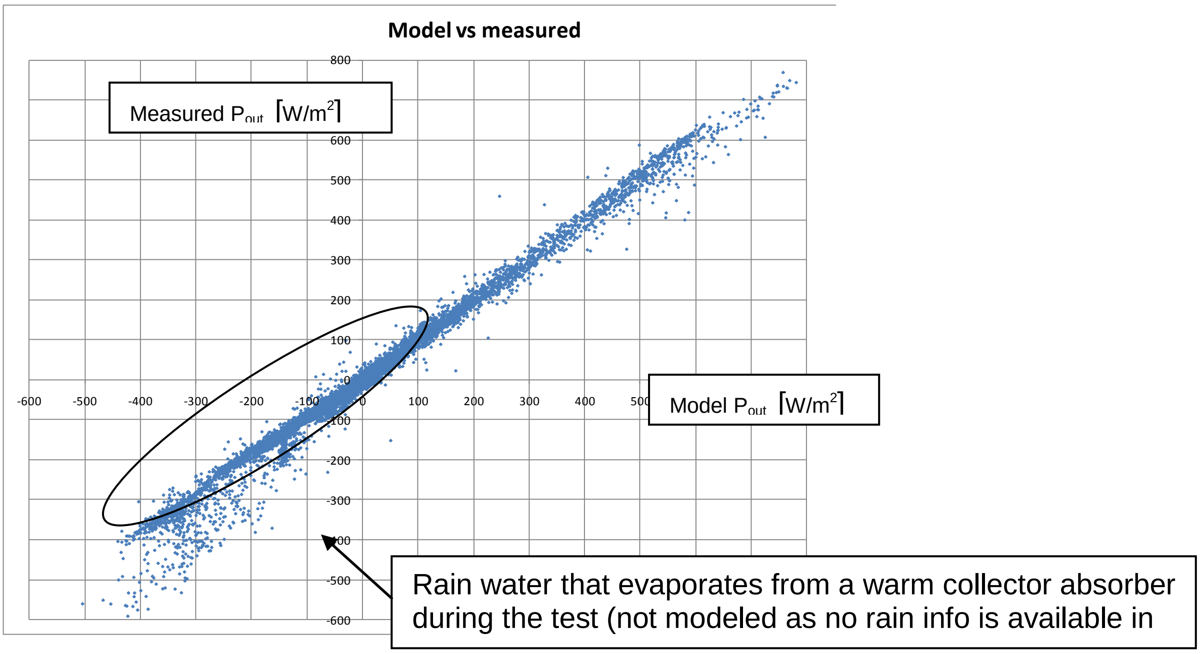

Figure 8. Data from 2010 09 08 until 2010 10 14. 5 minute average values. Data with and without condensation operation.

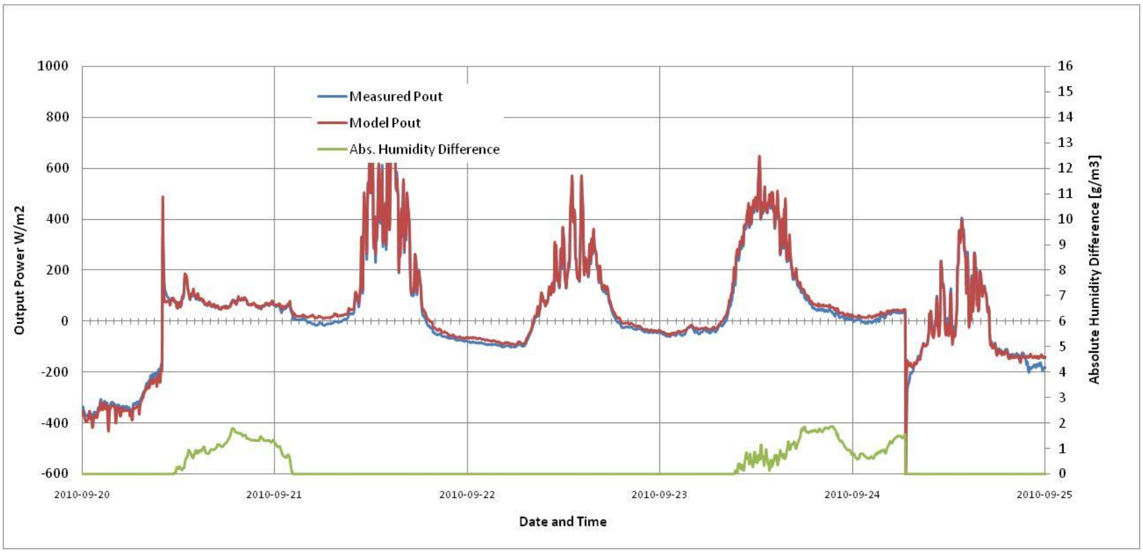

Figure 9. Results for the whole test period: Red= modeled Pout, Blue = measured Pout, Green= absolute humidity difference. High green values correspond to a large amount of condensation.

3.4 The model parameter values derived for the whole test period

The parameters and statistical results are summarized in numerical form in table 1.

Table 1. Output of Multiple regression analyze on all test data from September 8 until October 14. Both day and night = 24 hour operation.

Incidence angle curve for beam radiation and effective diffuse incidence angle modifier

SUMMARY OUTPUT

Regression Statistics	
Multiple F	0.992588
R Square	0.985231
Adjusted I	0.985113
Standard I	24.28287
Observati	10364

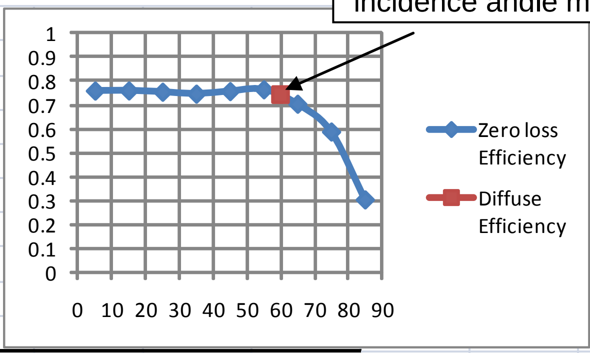

ANOVA

	df	SS	MS	F	gnificance F
Regressio	16	4.07E+08	25440107	43143.84	0
Residual	10348	6101780	589.6579		
Total	10364	4.13E+08			

Model Parameters from test

		Coefficients	tandard Err	t Stat	P-value	Lower 95%	Upper 95%	ower 95.0%	pper 95.0%
	Intercept	0	#N/A	#N/A	#N/A	#N/A	#N/A	#N/A	#N/A
a1(5)	X Variable	0.712947	0.019059	37.4075	2.3E-287	0.675588	0.750307	0.675588	0.750307
a1(15)	X Variable	0.760532	0.00427	178.0942	0	0.752161	0.768903	0.752161	0.768903
a1(25)	X Variable	0.75518	0.004216	179.1049	0	0.746915	0.763445	0.746915	0.763445
a1(35)	X Variable	0.747095	0.004942	151.1867	0	0.737409	0.756781	0.737409	0.756781
a1(45)	X Variable	0.757919	0.005601	135.3113	0	0.746939	0.768898	0.746939	0.768898
a1(55)	X Variable	0.765452	0.007324	104.5059	0	0.751094	0.779809	0.751094	0.779809
a1(65)	X Variable	0.704728	0.010371	67.94955	0	0.684398	0.725058	0.684398	0.725058
a1(75)	X Variable	0.588547	0.025987	22.64816	7E-111	0.537609	0.639486	0.537609	0.639486
a1(85)	X Variable	0.304363	0.153746	1.979642	0.04777	0.00299	0.605735	0.00299	0.605735
a2(Diffuse)	X Variable	0.743831	0.002783	267.3183	0	0.738377	0.749286	0.738377	0.749286
c1 (Convec)	X Variable	-11.6739	0.056009	-208.426	0	-11.7836	-11.5641	-11.7836	-11.5641
c3 (Wind)	X Variable	-4.03431	0.03964	-101.773	0	-4.11201	-3.95661	-4.11201	-3.95661
c5 (Dynam)	X Variable	-12831.5	185.1486	-69.3039	0	-13194.4	-12468.6	-13194.4	-12468.6
c4 (Longw)	X Variable	0.519665	0.009468	54.88474	0	0.501105	0.538225	0.501105	0.538225
c7(Conden)	X Variable	1210.659	58.88078	20.5612	4.17E-92	1095.242	1326.077	1095.242	1326.077
c6(W*Gtot)	X Variable	-0.03072	0.001271	-24.1658	1.5E-125	-0.03322	-0.02823	-0.03322	-0.02823

The parameters (called coefficients in table 1) in the collector model are within expected ranges from theory for this collector design. The total accuracy of the model is very good with a Multiple R of 0.99 and a standard deviation of 24 W/m2. This is in spite of no selection of data. All 5 minute average values available are used (over 10000 lines or time records of data).

The t-ratios (column "t Stat" above in table 1) are all much larger than 2 (with one exception a1(85) for 85 deg incidence angle) often more than 10 times lager. This indicates very reliable parameters and terms in the collector model. The a1(85) value has a lower t-ratio 1.97 At 85 deg incidence angle it is hard to determine the parameter and the alignment of the test rig and solar sensors are very critical. In many cases there are too few values available which cause this low t-ratio. The parameter a1(5) is also less well determined and the value is a bit lower than a1(15) which is not expected from the collector design. But here the problem is mainly that the sun is in this angular position (within 5 deg from the normal to the collector) very few if any hours during this period of the year. A change of the tracker tilt for a shorter period could probably have solved the weakness in this parameter. The two columns in table 1 to the right are repetitions of the two columns to the left of them. This is because no other confidence value than 95% was specified. If for example 90% would have been specified these columns would have had different values.

3.5 Explanation of the parameter values presented

a1(θ) = 0.30 - 0.76 (Zero loss or "optical" efficiency coefficient for beam solar radiation from θ = 5 deg incidence angle until θ = 85 deg).

a2= 0.74 (Zero loss or "optical" efficiency for diffuse solar radiation)

c1=11.7 W/m^2/K (Convective and radiation heat transfer coefficient at no wind)

c2=0.0 J/m^2/K^2 (Temperature dependence of the heat loss coefficient, This is set to zero here as the temperature variation in data is low and the Excel 2007 tool used here, could not handle enough parameters)

c3= 4.0 J/m^3/K (Wind dependence of the heat loss/gain)

c4=0.52 (Absorber effective emissivity for long wave radiation, includes inactive areas of the absorber) c5= 12830 J/m^2/K (Effective one node thermal capacitance)

c6=0.031 s/m (Wind dependence in zero loss efficiency)

c7=1211 (Condensation gain parameter. Ideally expected to be 1900 for a perfect flat absorber with a 100% wetted, active surface).

A note can be made that c1, c2 and c7 are active absorber surface area dependent. Therefore absorber surface enlargements (compared to the aperture or front area of the collector) with corrugations and/or individual pipes may improve the performance. These 3 parameters will then be increased in proportion to the surface area increase, compared to a flat absorber. This is taken into account in the TRNSYS model for the condensation term, as a separate input parameter. Also a double sided mounting arrangement "above the roof" of a flat absorber will give the same tendency.

4. TRNSYS model check with measured data

To be able to verify that the TRNSYS model is programmed correctly the measured collector model input data, from the test, was read into TRNSYS and the collector output was calculated/simulated, with the same collector parameters that were derived in the model validation.

Figure 10 shows the result for a few days with variable climate and operating temperatures. The TRNSYS model can follow the measured data in a good way, even if there are small deviations in the same order as in the Excel tool due to small imperfections in the model and for example missing information about rain. Of course also the inevitable measurement uncertainty will always add to the scatter.

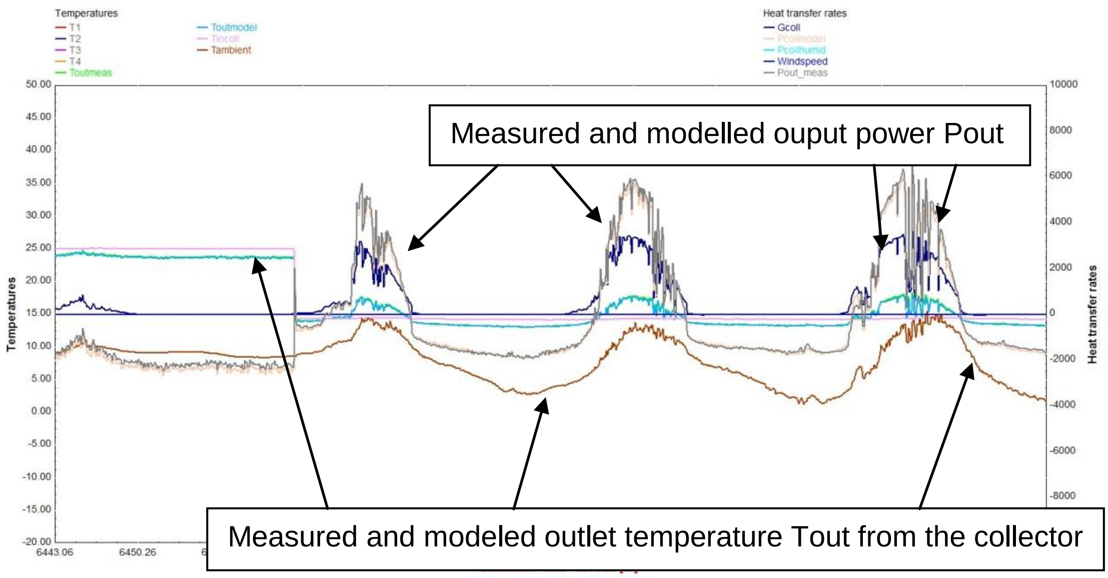

Fig 10. Output diagram from TRNSYS simulation with measured input data from the collector test. It can be seen that the simulation tool works as close as one can expect compared to both day and night measured data.

5. Comparison of TRNSYS versus IDA

ÅF is mostly working with the IDA software for system simulation and wanted to implement the model in their simulation system to be able to investigate for example recharging of large borehole systems with seasonal storage capacity. Therefore the proposed collector model was added to IDA and compared to TRNSYS for the same annual climate data and operating conditions, see table 2. The match was very good and the small difference come most probably from for example differences in how solar radiation is converted from climate data to a tilted collector area and also differences in how long wave sky radiation is treated. This could not be changed or synchronized. Therefore some small differences remains that are not caused by collector model errors or differences.

Tab. 2: Comparison of annual energy flows per m2 collector aperture area, between IDA and TRNSYS for the same climate data and model parameters. Main units are kWh/m2 and °C.

	TRNSYS				**IDA**			
Collector operating temperatur	Direct Solar Radiation	Diffuse Solar Radiation	**Collector Output**	**Condensation energy flow**	Direct Solar Radiation	Diffuse Solar Radiation	**Collector Output**	**Condensation energy flow**
0	609	573	**2400**	**254**	602	510	**2381**	**266**
5	609	573	**1537**	**123**	602	510	**1510**	**132**
10	609	573	**928**	**36**	602	510	**898**	**41**
15	609	573	**546**	**5**	602	510	**516**	**7**
20	609	573	**325**	**2**	602	510	**300**	**4**

To have a more detailed comparison, also some hourly values during 4 days are shown in figure 11 and 12 for the two softwares. Total collector output and the condensation energy contribution are shown separated. The match is satisfactory. A small time lag can be seen partly caused by the different definitions of time in IDA and TRNSYS.

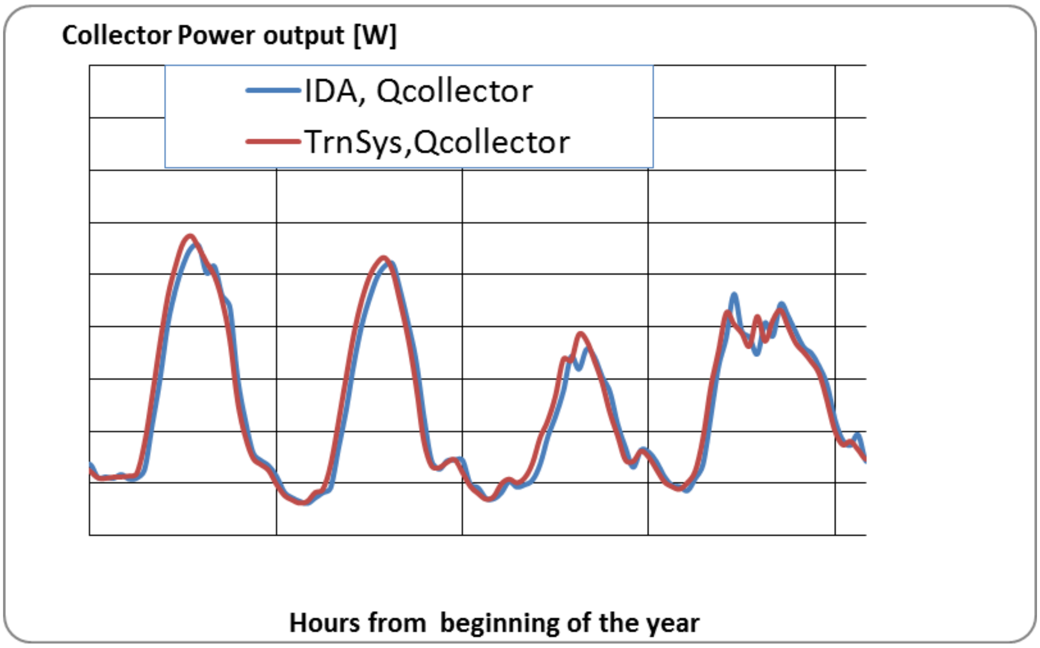

Figure 11. Comparison of collector putput power from TRNSYS and IDA for the same input parameters, operating condtions and climate.

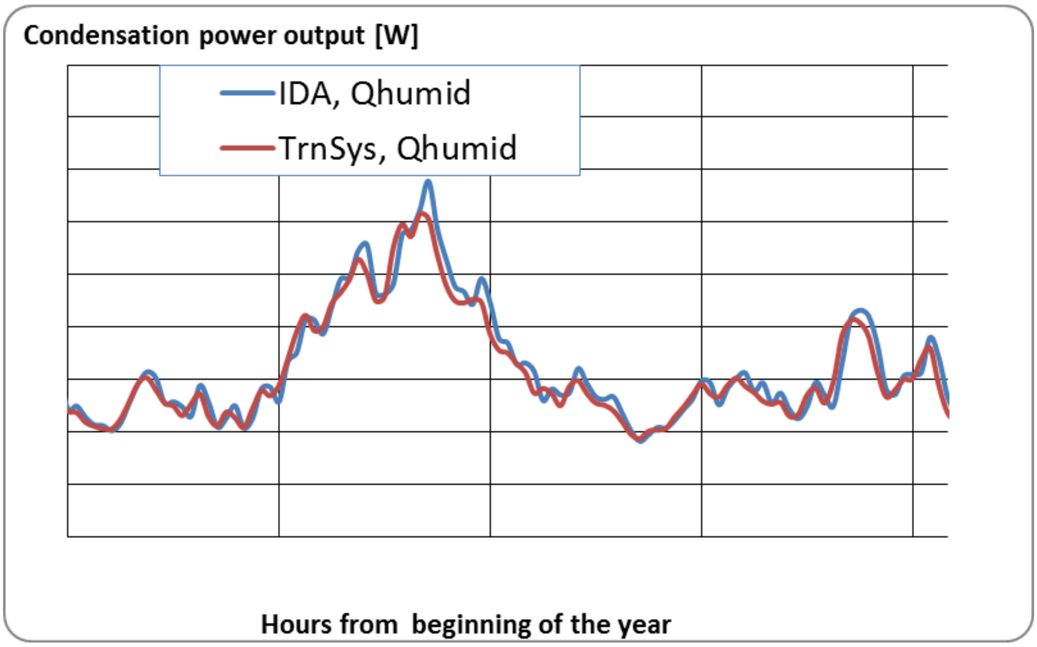

Figure 12. Comparison of collector putput power from TRNSYS and IDA for the same input parameters, operating condtions and climate.

6. Discussion and Conclusions

The model validation has shown that the extended EN12975 QDT (Quasi Dynamic Testing) model *in full dynamic application* can predict the output power of a flat plate unglazed collector very well also during low temperature operation when condensation add to the power output.

The model can also handle night time operation except when rain comes to a hot absorber and evaporation will occur and increase the heat loss. This can be handled with the model if information of rain is added in the measurements. (Operation with evaporation is only interesting for cooling applications.)

The parameter values derived are close to expected values even if the individual collector and absorber design will always shift the values somewhat. In this case the absorber has a quite uneven surface when filled with water. This will affect the surface boundary layer thickness and the parameters c1, c2 and c7. These parameters will also be affected by the inactive round welding “spots” (see figure 2 and 3) where no heat can be extracted to the fluid due to the low thermal conductivity of polymeric materials.

The extreme check of the model during 24 hour operation shows good agreement, except when there is rainwater on the absorber. (this can be deduced from the long wave net radiation that goes to zero with very thick clouds, as it is, only during rainy weather). This rainwater will evaporate from the absorber and reduce the output power in the opposite way as compared to condensation. Measurement of precipitation will make the test evaluation much easier and more accurate, if applied. The model can handle this if rain data is available.

Normally the collector will not be operated at negative output power in an application except for cooling purposes, so this is of a more academic and testing interest to shorten the testing time.

The heat transfer rate from condensation is limited and the convection heat transfer is most often larger (not shown in this summary but visible in the evaluation tool).

Therefore a more detailed modeling for the condensation than the one done here, is not necessary, if accuracy of the total collector output power is the main modeling goal.

Both convection and condensation heat transfer will increase with larger absorber surface area per m2 of aperture area. Therefore some kind of surface enlargement by corrugation of the surface, or a design with individual pipes, or even fins, are probably very favorable for this kind of collector. This is if it is used for operation at low temperatures together with a heat pump or for recharging a ground storage. This still needs more validation work that is discussed for the further validation of the model.

7. Acknowledgements

This work has been supported by ÅF infrastructure and especially thanks to Carina Martinsson ÅF for arranging with the project and leading the work from the ÅF side. Also thanks to Jim Fredin and Urban Cronström at IVT for early support with experimental installations for this modeling work at Lund University. Support from the European commission and the Swedish National Energy Administration made it possible to carry out collector performance tests at SP with additional advanced measurement equipment which was essential for the success of this work.

8. References

Perers B. A Dynamic Collector Model for Simulation of the operation below the dewpoint
in Heat Pump Systems. Eurosun Conference Glasgow (2006)

Perers B, Karlsson B, Kjellsson E, Hellström G. An Unglased Solar Collector model for the simulation of Ground Source Heat Pump Systems. North Sun 2005.

Kjellsson E. (2005) Solar Collectors and Ground Source Heat Pump in Combination. North Sun 2005.

Tepe R., Rönnelid M. and Perers B. 2003 Swedish Solar Systems in Combination with Heat Pumps. Proceeding from ISES Solar World Congress 14-19 June 2003. Göteborg, Sweden.

Kjellsson E. (2004) Solar Heating in Dwellings with Analysis of Combination of Solar Collectors and Ground Source Heat Pump (In Swedish). Report TVBH 3047 Dept of Building Physics Lund University Sweden 2004. www.byfy.lth.se/Publikationer/3000.html

Incropera , De Witt Fundamentals of heat and mass transfer. Page 352-357 + tables of properties. John Whiley & Sons 1990.

Nevander, Elmarsson. Fukthandboken ISBN 91-7332-716-6 page 236-241, 372-374.

Soltau, H. München 1989. Phd on unglased collectors. VDI Verlag. ISBN 3-18-143906-1 Page 64-72.

Personal Communication with Wolfgang Eisenmann ISFH Hameln Germany.

Pitz-Paal Robert. Kondensation an unabgedeckten sonnencollectoren. Diplomarbeit Ludvig Maximilians Universität München (1988)

Beckman W, Duffie J. Solar Engineering of Thermal Processes. ISBN 0-471-51056-4 (1991)

Sartori E. Convection Coefficient Equations for forced air over flat surfaces. Solar Energy 80 (2006) 1063-1071.

Perers, B. An improved Dynamic Solar Collector Model including Condensation and Asymmetric Incidence Angle Modifiers. Eurosun 2010.